Laser-induced Fluorescence Studies of Hematoporphyrin Derivative (hpd) In Normal and Tumor-tissue of Rat

Ankerst, J; Montan, Sune; Svanberg, Katarina; Svanberg, Sune

Published in:
Applied Spectroscopy

DOI:
10.1366/0003702844554738

1984

TABLE III. Analytical data for tungsten in tungsten concentrates and alloys.

			ICP-AES		Gravimetric/recommended		
		N	X	% RSD	X	S	% Diff[c]
NBS 277	W-concentrate	24[a]	53.35	0.24	53.45[b]	0.24	0.19
SYN 100	Quality control solution	5	99.97	0.11	100		0.03
SYN 80	Quality control solution	6	79.72	0.32	80		0.35
SYN 60	Quality control solution	5	60.23	0.17	60		−0.38
SYN 40	Quality control solution	6	40.32	0.35	40		−0.80
GSI 2	W-alloy	5	85.45	0.15	85.5		−0.06
GSI 4	W-alloy	5	74.6	0.3	73.9		−0.95
GSI 10	W-concentrate	5	34.3	0.10	33.6		−2.06

[a] Average value of data obtained by nebulizing the solution every 3 minutes, for more than one hour.
[b] Recommended value (see Ref. 16).
[c] Diff = (Recommended value − ICP value)/Recommended value × 100.

of 0.2% RSD and an accuracy of ±0.5 at the 90% W concentration level.

Decomposition and dissolution of the tungsten ores, alloys, and concentrates with sodium peroxide in pyrolytic crucibles is rapid, and the solutions produced are stable over extended periods of time. This dissolution technique, in combination with the high resolution spectrometer and the recognized benefits of the ICP, enables one to determine tungsten over a wide concentration range, thus overcoming the necessity of dilution. Furthermore, the same sample solution can be used for the determination of other major and minor constituents. This lends considerable flexibility to the proposed approach.

Due to the relative freedom from chemical interferences, matrix matching of standards to samples is avoided, and the only matrix matching required is the addition of NaCl and acid to the calibration standards.

In comparison to the gravimetric procedure, where time-consuming sample handling procedures can degrade the precision and the accuracy, the proposed ICP procedure is characterized by minimal handling procedures.

In conclusion, it can be stated that W can be determined in tungsten ores, concentrates, and alloys with high precision and accuracy with the use of ICP-AES and that this techinque can be considered as an alternative to the conventional gravimetric procedure.

1. Tungsten News, K. H. Miska, Ed. (Amax Inc., Greenwich, Connecticut, 1980).
2. J. J. Topping, Talanta, Mini review **25,** 61 (1978).
3. E. C. Sprenz and M. J. Prager, Analyst **106,** 1210 (1981).
4. G. Wünsch, Talanta **26,** 291 (1979).
5. N. Czech and G. Wünsch, Spectrochim. Acta. **36B,** 553 (1981).
6. A. J. Vogel, *Text Book of Quantitative Inorganic Analysis* (Longmans, London, 1961).
7. P. W. J. M. Boumans, Fresenius Z. Anal. Chem. **299,** 337 (1979).
8. S. Greenfield, Analyst **105,** 1032 (1980).
9. J. Dolezal, P. Povondra, and Z. Sulcek, *Decomposition Techniques in Inorganic Analysis* (Elsevier, New York, 1968).
10. Z. Sulcek, P. Povondra, and J. Dolezal, CRC Critical Rev. in Anal. Chem. **6,** 255 (1977).
11. W. W. Scott and N. H. Furman, *Standard Methods of Chemical Analysis* (Von Nostrand, New York, 1939).
12. P. Tekula-Buksbaum, Microchim. Acta **1,** 145 (1977).
13. J. M. Mermet and C. Trassy, Appl. Spectrosc. **31,** 237 (1977).
14. G. J. Schmidt and W. Slavin. Anal. Chem. **54,** 2491 (1982).
15. I. B. Brenner, H. Eldad, S. Erlich, and N. Dalman, "Application of ICP-AES and an Internal Reference for the Direct Determination of Sulfate and Calcium in Waters and Brines," in press, Anal. Chim. Acta, 1984.
16. National Bureau of Standard certificate for NBS 277.

Laser-Induced Fluorescence Studies of Hematoporphyrin Derivative (HPD) in Normal and Tumor Tissue of Rat

J. ANKERST, S. MONTÁN, K. SVANBERG, and S. SVANBERG

Department of Physics, Lund Institute of Technology, P.O. Box 725, S-220 07 Lund, Sweden (S.M., S.S.); and Lund University Hospital, S-221 85 Lund, Sweden (J.A., K.S.)

Fluorescence studies of hematoporphyrin derivative (HPD) in normal and tumor tissue of rat were performed with nitrogen laser excitation and optical multi-channel detection. Fifteen types of tissue including inoculated tumor were investigated for rats at different delays after HPD injection. Optimum contrast functions and other criteria for discriminating tumor tissue from normal tissue are discussed. The results should have implications for practical human HPD endoscopy.

Index Headings: **Fluorescence; Techniques, spectroscopic.**

Received 3 December 1983; revision received 1 February 1984.

INTRODUCTION

During the last few years, tumor localization and treatment based on hematoporphyrin derivative (HPD) administration combined with light radiation has received considerable attention. While some of the tumor-seeking and photodynamic properties of certain photosensitizers have been known for quite some time, the great potential of the techniques has become apparent more recently. Many groups, in particular the one of T.J.

0003-7028/84/3806-0890$2.00/0

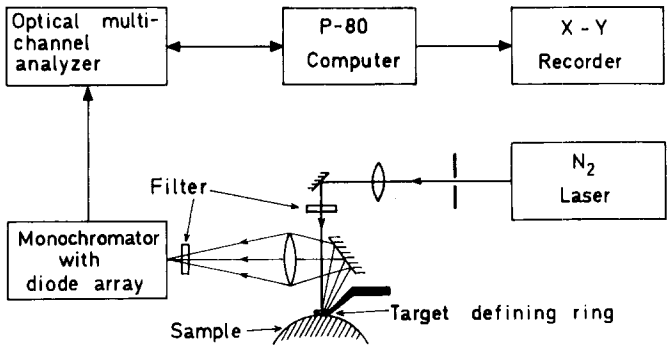

FIG. 1. Experimental arrangement for laser-induced fluorescence measurements in tissue.

Dougherty at Roswell Park Memorial Institute, have contributed to the development of the field. An authoritative review of the work in the area has been prepared by Dougherty.[1] In two specialized recent conferences,[2,3] the research around HPD has been covered. A literature survey of the field has been made by two of us.[4]

The progress in the HPD field has been connected with the establishment of well characterized HPD preparations and the remarkable progress in applicable laser technology. Very recently, the most active component of HPD has been identified as di-hematoporphyrin ether (DHE).[1]

Hematoporphyrin Derivative Photodynamic Therapy (HPD-PDT) relies on the necrosis of tumor tissue as normal triplet oxygen is transferred to cytotoxic singlet oxygen through a reaction with photo-excited HPD molecules. Selective uptake and/or retention of HPD in tumors results in a higher therapeutic ratio than normally available with other modalities for cancer treatment. The penetration of light through tissue is a critical parameter that has been investigated by Dougherty *et al.*[5] and more recently by Svaasand *et al.* and others.[2,3] At 630 nm, a penetration depth of 5–20 mm is obtained, while the HPD molecules can still be efficiently excited. For cutaneous tumors, properly filtered lamps or lasers close to 630 nm can be used; whereas for endoscopic applications or deeper subcutaneous lesions, laser light delivered by fiber optical systems is preferred. Presently, CW argon-ion laser pumped dye lasers (0.5–4 W) are the most common systems, whereas fixed-frequency pulsed gold-vapor lasers (628 nm) seem to be evolving into an attractive alternative.

Presently, about two dozen groups are involved in more or less extensive HPD programs. Several larger clinical tests have been reported, e.g., by Dougherty *et al.*,[5] Wile *et al.*,[6] Forbes *et al.*,[7] Hayata *et al.*,[8] and Cortese *et al.*[9] Particularly for small lesions, the therapeutic results are very encouraging.

Whereas HPD photodynamic cancer treatment is a very exciting and rapidly developing possibility, this is not the only aspect of HPD in connection with the management of malignancies. Upon excitation in the Soret band, peaking at 404 nm, HPD exhibits very characteristic dual-peaked fluorescence in the red spectral region. In connection with the tumor-seeking properties of HPD, this fluorescence is being used for tumor localization, particularly for lung[10,11] and bladder[12] malignancies.

Normal endoscopic systems supplemented with a fluorescence detection capability have been constructed,[13] as well as more advanced imaging fluorescence equipment.[14] The optimal utilization of the HPD fluorescence signature in tissue is a topic of considerable importance for small tumor detection, irradiation dosimetry, and general guidance for the PDT personnel. The present paper addresses these questions in model experiments on HPD-injected rats with induced cancer tumors. The work is based on previous laser-induced fluorescence experience in remote sensing,[15] industrial surface cleanliness monitoring,[16] and non-HPD tissue investigations.[17,18]

MATERIALS AND METHODS

In the present investigation of laser-induced fluorescence in tissue, white inbred female Wistar/Furth (W-Fu) rats of weight around 250 g were used. A malignant tumor on the outside of the right hind leg had been induced by local inoculation of syngeneic tumor cells prepared from a colon adenocarcinoma (DMH-W49).[19] The original colon tumor was induced by subcutaneous injections of 1,2-dimethylhydrazine and passaged in W-Fu rats. At the time of animal sacrifice and fluorescence investigation (21 days after tumor inoculation) the tumors were about 25 mm in diameter. One to four days before the investigation, the rats had been injected intravenously (left v. femoralis) at a level of 5 mg/kg body weight by 0.5 mg/mL HPD solution (Photofrin I solution, ORD Inc., Cheektowaga, N.Y., diluted 10 times in physiological saline).

In Fig. 1, the set-up used for laser-induced fluorescence studies is shown. As an excitation source, we used a nitrogen laser emitting at 337.1 nm. The laser was operated at a repetition rate of 10 Hz with a pulse duration of about 10 ns. A 340-nm interference filter of 10-nm bandpass was used in the excitation beam to eliminate unwanted plasma lines. The light impinging on the target had a peak power of about 3 kW and had a circular diameter of about 3 mm. The interaction spot was defined by a fixed metal ring of about 10-mm diameter, in which the laser light was centered. From below, the target tissue was pressed towards the ring. In one measurement series, a thin, flat, fluorescence-free quartz plate was placed below the ring for still better definition of the target position. Fluorescence light released from the irradiated tissue was reflected horizontally by a flat, first-surface aluminized mirror and was focused with a d = 10 cm, f = 15 cm quartz lens towards the 0.2-mm entrance slit of a Tracor Northern IDARSS optical multichannel analyzer system. In the focal plane of a Jobin Yvon UFS-200 spectrograph, a TN-1223-4IG intensified diode array detector was placed. With a dispersion of 24 nm/mm the entire near-UV-visible/near-IR spectrum could be captured with the 1024-element, 25-mm diode-array detector assembly. Each of the diodes can be read out to the TN-1710 mainframe, where the full spectrum is immediately available for display on the CRT screen. For reasonably strong fluorescence signals, a spectrum can be captured with the use of a single 10-ns laser pulse. Diode arrays have a certain dark-current signal, which can be compensated for by the subtraction of the signal for the same number of blocked laser pulses. This pro-

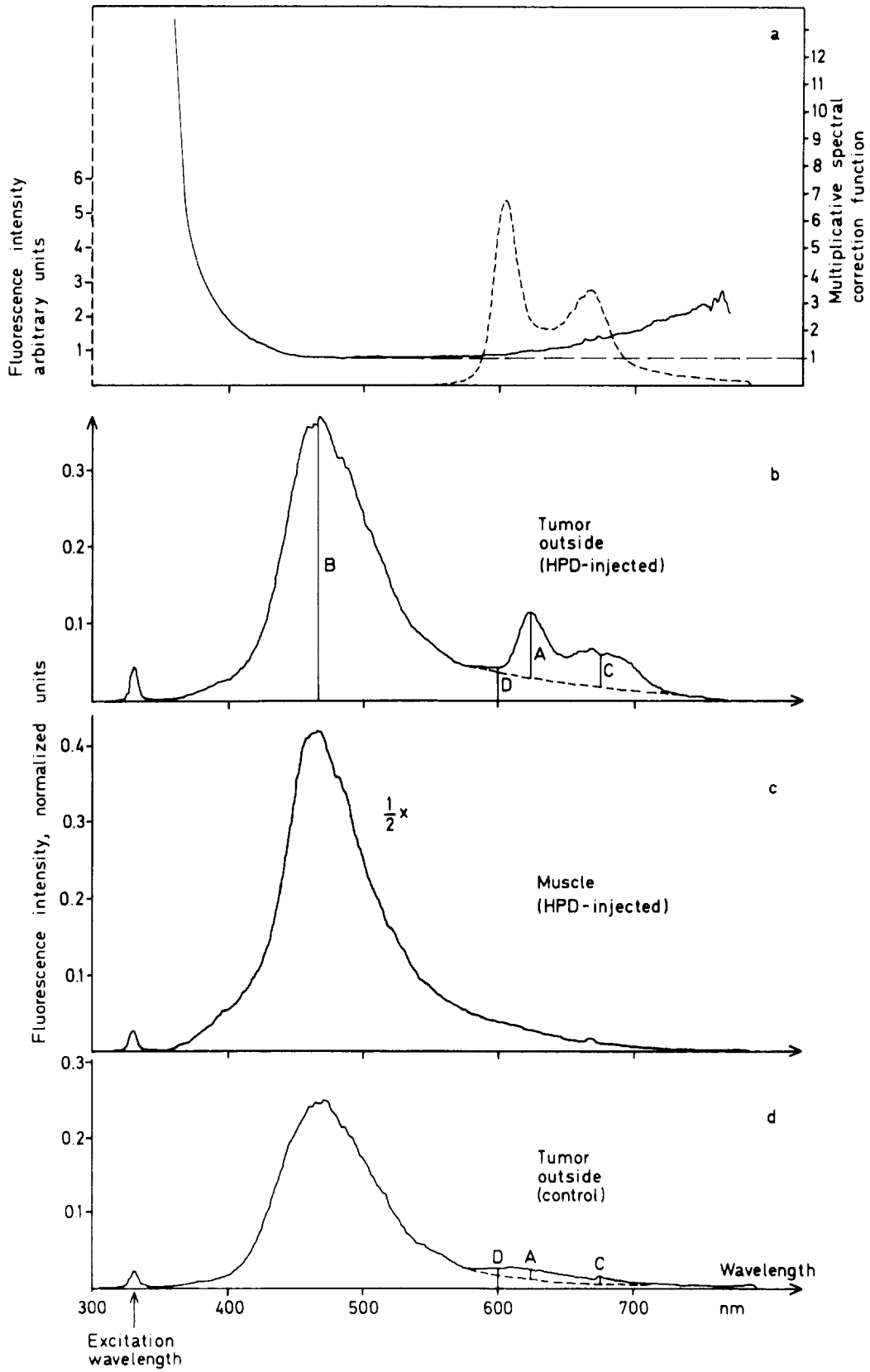

FIG. 2. a, Fluorescence spectrum of diluted Photofrin solution (broken line). Spectral correction factor (full line). b, Fluorescence spectrum of tumor surface for a rat that had been injected with HPD two days earlier. Signal intensities at characteristic wavelengths are denoted by A, B, C, and D. c, Fluorescence spectrum of muscle on unaffected leg for the same rat as in (b). Note that the curve has been reduced by a factor of 2. d, Fluorescence spectrum of a tumor for a rat that did not receive an HPD-injection.

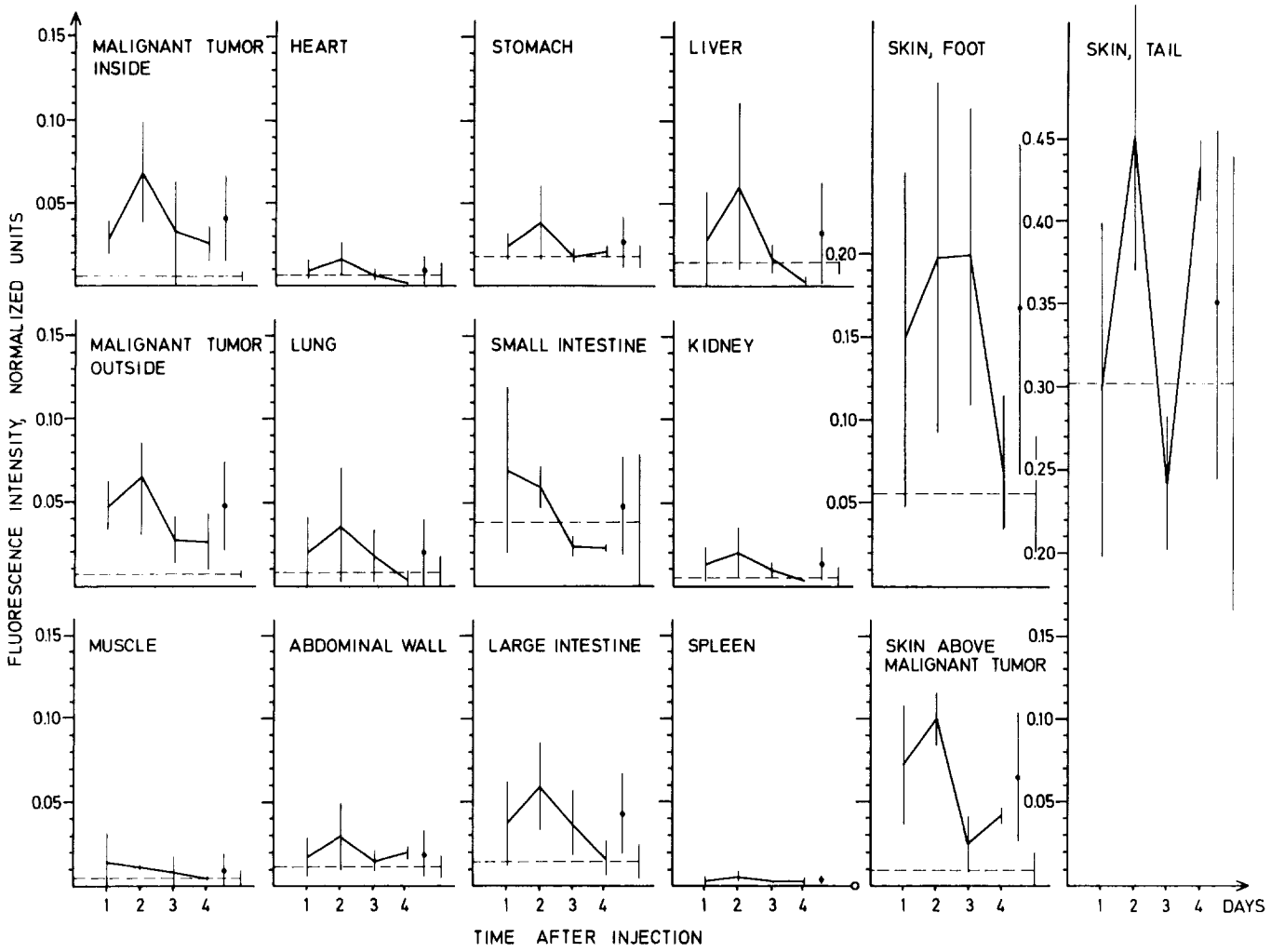

FIG. 3. Fluorescence intensity A in normalized units for different rat tissues. Intensities are shown with standard deviations for different times after injection. To the right of the 4 points, the mean value with error bars is shown, disregarding any temporal evolution. Further, the background level for noninjected rats is also indicated with a broken line and error bars. When the background level is zero, this has been indicated with a ring on the horizontal axis.

cedure was always used in the measurements. By the use of a calibrated tungsten lamp, the spectral response of the spectroscopic system has been calibrated and the corresponding correction function has been stored in the minicomputer attached to the Tracor-Northern mainframe. Measured spectra together with proper identification information were transferred to the floppy disc unit of the minicomputer. We used a P-80 minicomputer in our experiments. In the computer, the spectra could be analyzed with the use of appropriate software (to be described in a forthcoming paper[20]). The spectra could also be read out on a x-y recorder. In the present investigation, all data were derived in manual evaluations to gain maximum insight into the fluorescence features.

MEASUREMENTS AND RESULTS

Measurements were performed in two experiment series, each containing ten animals. In one series, two or three rats were injected 1, 2, or 3 days prior to investigation; whereas in the other series, two rats were injected 1, 2, 3, or 4 days before the measurements. Each series contained two control animals to which HPD had not been administered. In each series, the measurements were performed consecutively on all the animals with the use of an unaltered experimental set up. As a fluorescence standard, we used a 3-mm-thick layer of Rhodamine 6G dye in water (70 μg/liter). All measured fluorescence intensities are expressed in this unit. Other standards, like pieces of standardized white paper, were found to be inadequate, due to bleaching. The calibration dye solution was kept in small, nonfluorescent aluminum cups just below the target-defining ring. The detection system was checked for linearity with the use of calibrated neutral density filters.

For the measurements, the abdomen of the sacrificed rats was cut open, the individual organs *in situ* were pressed from below towards the ring, and data were accumulated for 50 laser pulses; background counts were likewise recorded for 50 pulses. Reference spectra were regularly recorded. The ring was carefully rinsed with ethanol between measurements as needed. Spectra for heart, lung, abdominal wall, stomach, small and large intestine, liver, kidney, spleen, skin (foot), and skin (tail)

TABLE I. Ratio C/A between the fluorescence intensities of different tissues at 675 and at the red main peak around 630 nm. Values are mean values for rats injected 1-4 days prior to examination. The standard deviation is indicated.

Tissue	C/A
Malignant tumor (inside)	0.64 (8)
Malignant tumor (outside)	0.57 (6)
Liver	0.43 (13)
Lung	0.33 (8)
Skin, foot	0.30 (10)
Skin, tail	0.20 (5)
Small intestine	0.27 (12)
Large intestine	0.20 (4)
Feces	0.27 (6)

were recorded for unperturbed organs. The tumors were investigated as follows: First, the skin above the shaved tumor was measured, then the skin was removed by a scalpel to expose the tumor capsule, and finally the tumor was cut open and the interior tissue was investigated. A spectrum from the exposed fascia of the muscle at the tumor location on the healthy hind leg was also recorded for reference.

In Fig. 2, the types of spectra recorded in the present investigation are shown. In Fig. 2a, the fluorescence spectrum of a layer of Photofrin solution diluted 100 times in 0.9% saline is shown. A characteristic dual-peaked spectrum (~610 and ~670 nm) is obtained.

In Fig. 2a, an experimentally determined spectral correction curve is also shown. By the use of this curve, all data in the present paper can be recalculated to the case of a flat spectral response. As can be seen, the curves are particularly influenced in the short wavelength region where the GG 375 laser blocking filter partially absorbs. In Fig. 2b, the spectrum from the tumor surface of a rat, injected 2 days earlier, is shown featuring very clear HPD fluorescence. The first peak has been shifted to longer wavelengths (~630 nm) and the second peak has broadened. Similar observations have been made in Ref. 21. Signal intensities at characteristic points have been denoted by A, B, C, and D. For comparison, a corresponding spectrum from the other leg of the same rat is shown in Fig. 2c. As can be seen, the amount of characteristic HPD fluorescence is here very small, demonstrating the HPD differentiation. However, it should be noted that the amount of nonspecific red fluorescence, as would be observed through a filter transmitting above 600 nm, is substantial; by just observing red fluorescence without considering the specific HPD signature, ones differentiation would be poor. In Fig. 2d, the spectrum of the tumor surface of a non-injected rat is shown. This spectrum should be compared with the one in Fig. 2b. As can be seen, some red fluorescence above a smoothly falling off background exists. However, it does not exhibit the specific HPD features. As an indicator of HPD uptake, we have measured the height A of the major read peak above a smoothly falling background in terms of the fluorescence standard as discussed above. Also for cases where HPD is absent, as in the control rats (e.g., Fig. 2d), or when the signature is unclear, we have measured the value of A above the background at 630 nm. The results with standard deviations are plotted in Fig.

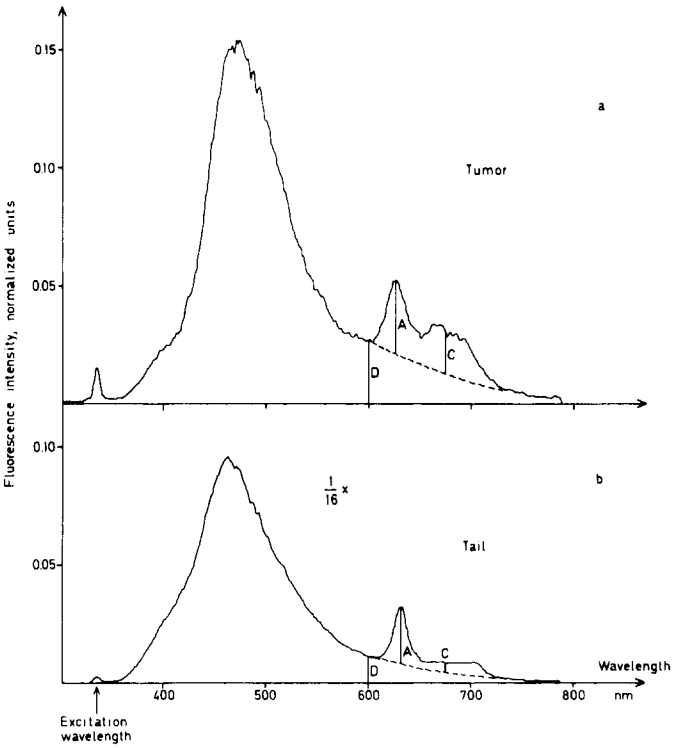

FIG. 4. Comparison between fluorescence spectra for tumor interior (a) and tail skin (b). Note that the tail spectrum is reduced by a factor 1/16.

3 as a function of time from HPD administration. For each organ, the value for the control rats (no HPD administration) is indicated as a dashed line. Normally, the values are based on measurements on four animals.

Although the scatter in the data is rather large, some observations can easily be made. Over the studied period of time, some fall off in fluorescence intensity is noted for the studied rat tissues. Selective uptake in different organs as well as selective retention are important. Disregarding any temporal variation, the mean value (●) with standard deviation for all the injected rats is indicated in each diagram. A significantly stronger signal is obtained for the HPD-injected rats as compared with the control values for the different tumor tissues. Most important, the tumor tissues have a much higher HPD fluorescence than the unaffected muscle tissue, which is the HPD differentiation effect already evident in Fig. 2. On the other hand, strong signals are also obtained for, in particular, the skin of the foot and the tail, but also for the liver and the intestines. In separate tests, it was found that the intestine fluorescence largely originates from feces. In other separate tests on live injected rats, it was found that strong red fluorescence was obtained from the uncovered nose, ears, feet, tail, and feces, when observed through a Schott OG 590 filter transmitting light above 600 nm. The fluorescence was induced with the violet lines 407, 413, and 415 nm from a krypton-ion laser equipped with a fiberoptic output. As can be seen from the level in the control animals, most of the non-tumor skin fluorescence is due to naturally occurring constituents. In Fig. 4, the fluorescence spectrum from the tail skin is compared with the fluorescence from the

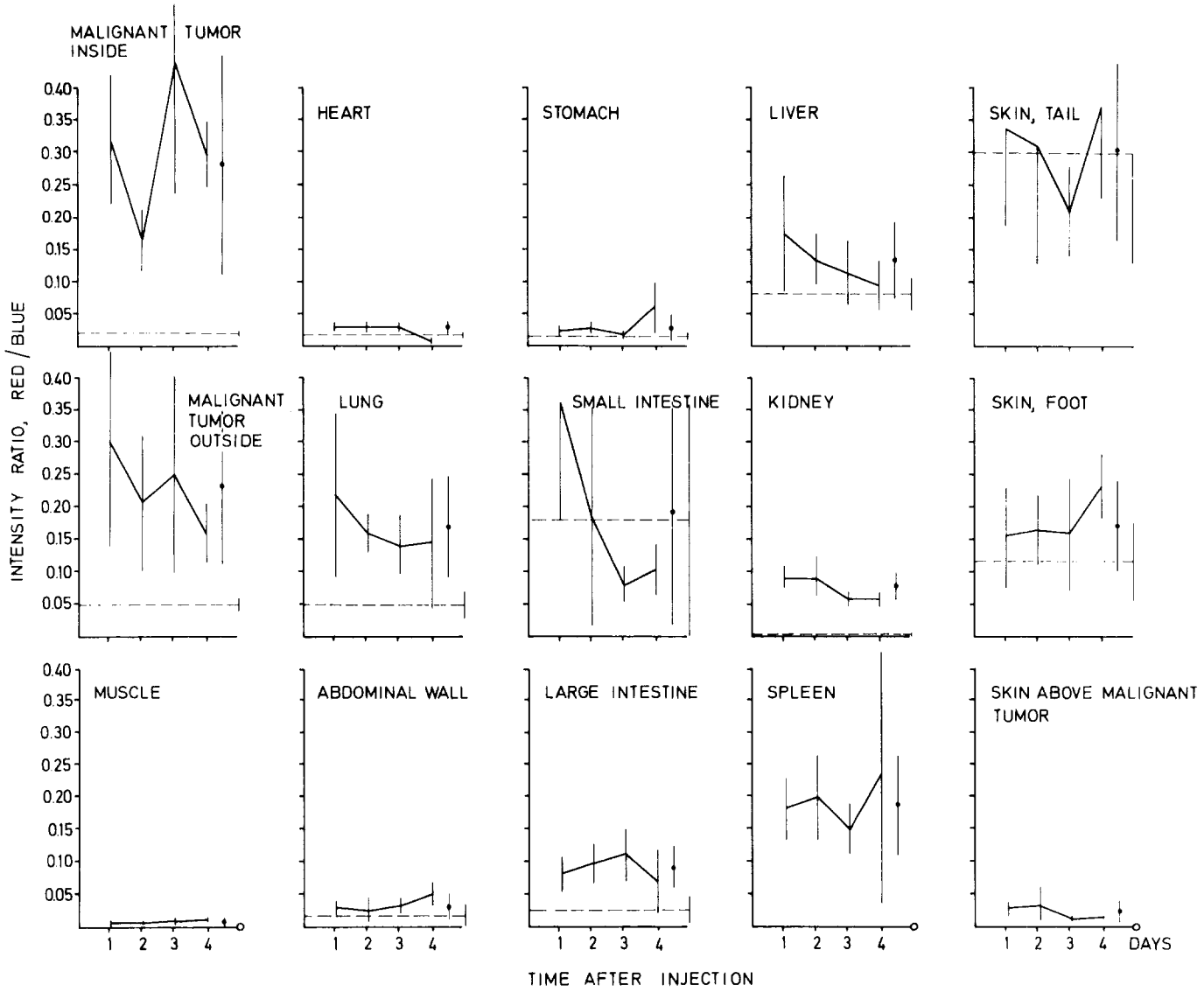

FIG. 5. Ratio of signal intensities A and B (red/blue). The plot has been made in a way similar to that in Fig. 3.

interior of a tumor in a rat injected 2 days earlier. We observe that the short-wavelength red peak of the skin is very prominent but narrower and shifted to ~635 nm. In Fig. 3, the height of this peak has been evaluated as the signal A, although the peak is not exactly at 630 nm. From Fig. 4, it is also evident that the signal farther out in the red is very different for HPD-bearing tissue and the naturally red-fluorescing tissue, as, e.g., measured at 675 nm (signal C). It should be noted that the grating second-order signal at 674 nm due to the exciting light must be eliminated. In Table I, the values of C/A are listed with standard deviations for all the tissues with a high A-value. The values are averages independent of time. As can be seen, the ratio C/A is larger than 0.5 for tumor tissue and smaller than 0.3 for the naturally occurring red-fluorescing constituents. The lung and the intestines have lower ratios than tumor tissue. The intestine ratio is related to the low value for feces (0.27) found in separate measurements. For a set discrimination ratio of 0.5, only liver tissue occasionally falls in the same category as tumor tissue.

In the measurements, it was noted that the blue fluorescence intensity was considerably weaker in cancer tissue as compared to normal muscle tissue. This can already be observed in Fig. 2 at the blue peak at about 470 nm, intensity B. Thus, contrast between the two types of tissue can be enhanced by the formation of the ratio A/B. In Fig. 5, this ratio, which in the same way as the C/A ratio has the convenience of being free from the need of any intensity calibration, is plotted for the same rat organs as in Fig. 3 with standard deviations and control ratio levels. Indeed, a very good discrimination between tumor and normal muscle tissue is obtained, as seen in the left part of the figure. However, several other organs also have a high ratio. The very opaque organs like the kidneys and the spleen have low A-values, although they are known to have high HPD concentrations.[22,23] In the ratio A/B, the opacity influence is reduced. It should be noted that despite the shaving, the skin above the malignant tumor (lower right) has a small A/B ratio, due to excessive blue fluorescence in residual white hair coverage.

For discriminating tumor tissue from other tissue, it is desirable to form an optimum contrast function. By a careful comparison of Figs. 3 and 5, it is observed that increased contrast can be obtained, especially between tumor tissue and normal muscle, by the multiplying of the two types of diagrams by each other, i.e., to form the function A^2/B. High values for A^2/B are obtained only for the tumor tissue and for the lung, liver, intestines, foot, and tail skin. However, the non-tumor tissues, in particular the latter ones, show a high inherent fluorescence with "wrong" C/A ratio. The contrast advantage for A^2/B is reduced by the necessity of having an intensity calibration. By simultaneously requiring $A^2/B > 0.006$ (or $A/B > 0.15$) and $C/A > 0.5$, one can distinguish tumor tissue efficiently.

DISCUSSION

In this paper, we have emphasized the full utilization of the HPD fluorescence signature. Whereas better contrast can be obtained in human tissue, it was evident in the present studies on rat tissues that by merely measuring the integrated red light intensity for $\lambda > 600$ nm, very little information (differentiation) could be gained. Actually, when violet light from a krypton-ion laser was fiberoptically directed into the opened abdomens of rats and observation followed through a OG 590 filter, most organs looked, on visual inspection, rather undifferentiated red. By electronically monitoring a contrast function such as A/B or A^2/B, assisted by a reject criterion of the C/A type, one can obtain improved information for localizing and demarcating tumors. In endoscopic applications, especially, improved performance can be expected. It should be noted that other contrast functions may prove more powerful. With a computer-assisted, spectrally resolving system, the most useful response can be programmed. In the present investigation, we have used an expensive optical multichannel system yielding full spectral information. However, by the use of dichroic beamsplitters combined with filters of optimum halfwidth, the fluorescence light can be divided up into a low number of channels, corresponding, for instance, to A, B, C, or D. As a matter of fact, a 3-channel system, incorporating a nitrogen laser and a microcomputer, is presently being assembled,[24] primarily intended for industrial surveillance and process steering.

The HPD-related fluorescence monitored in this work cannot readily be used for assessing the HPD concentration. This is because of strong matrix effects; e.g., the opacity of different types of tissue varies greatly and fluorescence quenching may also vary. From studies with radioactively labelled HPD, quite a lot is known about the distribution of HPD in mice.[1,22,23] Thus liver, kidney, and spleen have very high levels; tumor, skin, and lung have intermediate levels; whereas muscle has low and brain and eye very low levels. By the application of suitable organ-specific correction factors, fluorescence may be useful for quantitative HPD assessments. The great advantage of the fluorescence technique is that it can be used for noncontact, immediate measurements without influencing the tissue. Specifically, by the optimization of the contrast between tumor tissue and normal surrounding tissue along the lines presented in this paper, otherwise occult cancers should be detectable and be made accessible for normal biopsy.

ACKNOWLEDGMENTS

Valuable discussions with Dr. T. J. Dougherty and Dr. M. W. Berns are gratefully acknowledged as well as the support and encouragement by the Lund HPD group, in particular professors A. Gustafson and D. Killander. The technical support by Å Bergquist and E. Gynnstam is much appreciated.

1. T. J. Dougherty, CRC Critical Reviews in *Oncology/Hematology*, S. Davis, Ed. (CRC Press, Florida, 1984).
2. Proc. of the Symposium on Porphyrin Localization and Treatment of Tumors, D. R. Doiron, Ed., Santa Barbara, California, April 24–28, 1983.
3. Proc. of the International Symposium on Porphyrins in Tumor Phototherapy, R. Cubeddu, Ed., Milano, Italy, May 26–28, 1983.
4. K. Svanberg and S. Svanberg, Lund Reports on Atomic Physics LRAP-23 (1983).
5. T. J. Dougherty, J. E. Kaufman, J. E. Goldfarb, K. R. Weishaupt, D. Boyle, and A. Mittleman, Cancer Res. **38,** 2628 (1978).
6. A. G. Wile, A. Dahlman, R. G. Burns, and M. W. Berns, Lasers in Surg. and Med. **2,** 163 (1982).
7. I. J. Forbes, P. A. Cowled, A. S.-Y. Leong, A. D. Ward, R. B. Black, A. J. Blake, and F. J. Jacka, Med. J. Aust. **2,** 489 (1980).
8. Y. Hayata, H. Kato, C. Konaka, J. Ono, and T. Tahizawa, Chest **81,** 269 (1982).
9. D. Cortese and J. H. Kinsey, Mayo Clin. Proc. **57,** 543 (1982).
10. J. H. Kinsey, D. A. Cortese, and D. R. Sanderson, Mayo Clin. Proc. **53,** 594 (1978).
11. E. G. King, G. Man, J. le Riche, R. Amy, A. E. Profio, and D. R. Doiron, Cancer **49,** 777 (1982).
12. A. Tsuchiya, N. Obara, M. Miwa, T. Ohi, H. Kato, and Y. Hayata, J. Urol. **130,** 79 (1983).
13. J. H. Kinsey and D. A. Cortese, Rev. Sci. Instr. **51,** 1403 (1980).
14. D. R. Doiron, E. Profio, R. G. Vincent, and T. J. Dougherty, Chest **76,** 27 (1979).
15. L. Celander, K. Fredriksson, B. Galle, and S. Svanberg, Göteborg Institute of Physics Reports GIPR-149 (1978).
16. P. Herder, T. Olsson, E. Sjöblom, and S. Svanberg, Lund Reports on Atomic Physics LRAP-9 (1981).
17. S. Montán, Lund Reports on Atomic Physics LRAP-17 (1982).
18. S. Montán, K. Svanberg, and S. Svanberg, unpublished results.
19. G. Hedlund and H. O. Sjögren, Int. J. Cancer **26,** 71 (1980).
20. S. Montán, unpublished results.
21. M. W. Berns, A. Dahlman, F. M. Johnson, R. Burns, D. Sperling, M. Guiltinan, A. Siemens, R. Walter, W. Wright, M. Hammer-Wilson, and A. Wile, Cancer Res. **42,** 2325 (1982).
22. C. J. Gomer and T. J. Dougherty, Cancer Res. **39,** 146 (1979).
23. C. J. Gomer, N. Rucker, C. Mark, W. F. Benedict, and A. L. Murphee, Invest. Ophthalmol. Vis. Sci. **22,** 118 (1982).
24. S. Montán and S. Svanberg, unpublished results.